Correlation Between Hyperreflective Foci in the Choroid and Choroidal Discoloration in Vogt-Koyanagi-Harada Disease

Young Ho Kim, Ariunaa Togloom, and Jaeryung Oh

Department of Ophthalmology, Korea University College of Medicine, Seoul, Korea

Correspondence: Jaeryung Oh, Department of Ophthalmology, Korea University Medicine, 73 Goryeodae-ro Sungbuk-ku, Seoul 02841, Korea; ojr4991@korea.ac.kr; ojr4991@yahoo.co.kr.

Received: February 16, 2022
Accepted: August 1, 2022
Published: August 25, 2022

Citation: Kim YH, Togloom A, Oh J. Correlation between hyperreflective foci in the choroid and choroidal discoloration in Vogt-Koyanagi-Harada disease. *Invest Ophthalmol Vis Sci.* 2022;63(9):27. https://doi.org/10.1167/iovs.63.9.27

Purpose. To investigate the distribution of hyperreflective choroidal foci (HCF) in eyes with Vogt-Koyanagi-Harada (VKH) disease.

Methods. We included 22 eyes of 11 patients with VKH disease in the convalescent stages and 22 eyes of age- and sex-matched normal controls. HCF were quantified using en face optical coherence tomography (OCT) images of the choroid, and the degree of fundus pigmentation was determined by the color balance of the fundus photographs. The results were then analyzed between the eyes with and without sunset glow fundus (SGF).

Results. The median age of patients with VKH disease was 58.0 (range 54.0–65.0) years, and median disease duration was 66.4 (range 8.5–147.7) months. In 22 eyes with VKH, the number and total area of HCF were correlated with the degree of fundus pigmentation ($\rho = -0.671$, $P < 0.001$; $\rho = -0.612$, $P = 0.002$, respectively). The number of HCF was significantly smaller in VKH disease–affected eyes with SGF (median, interquartile range; 134.6, 110.0–159.2) than in those without SGF (229.0, 197.0–261.0) and the eyes of normal controls (211.8, 190.3–233.4).

Conclusions. HCF distributions correlated with the degree of fundus pigmentation in eyes with VKH disease. Quantitative measurements of HCF on en face OCT images can be a novel tool in evaluating choroidal pigmentation in patients with VKH disease.

Keywords: choroid, hyperreflective foci, optical coherence tomography, pigmentation, melanin, Vogt-Koyanagi-Harada disease

Vogt-Koyanagi-Harada (VKH) disease is a multisystemic disease characterized by a granulomatous inflammation that affects the eyes, ears, meninges, skin, and hair.[1–3] Recent advances in optical coherence tomography (OCT) have provided detailed images of the choroid in vivo.[4] In addition to changes in the retinal layers such as bacillary layer detachment, changes in the vascular component of the choroid have been reported in eyes with acute and chronic VKH disease using OCT and OCT angiography.[5–7]

VKH disease is caused by an autoimmune reaction against melanocytes, which express tyrosinase family proteins and choroidal involvement of the disease has been reported in various studies.[1–3,8–10] Cellular involvement in VKH disease such as melanocytes has been elucidated in previous studies with pathologic specimens.[3,8,9] Previous studies using OCT have shown the possibility of delineation of chorioretinal cellular components such as hyperreflective foci.[11–14] In addition to normal eyes, hyperreflective foci have been presented in the retina or choroid of eyes with various diseases including diabetic retinopathy,[14,15] age-related macular degeneration,[16] and choroideremia.[13] It has been reported that they are related to disease activity,[17] as well as progression.[16] In recent studies,[18,19] using a quantitative measurement method of hyperreflective choroidal foci (HCF) on en face OCT, HCF were suggested to originate from pigmentation of melanocytes in the normal choroid.

Changes in choroidal components such as melanin pigment may be related to characteristic findings in VKH disease such as sunset glow fundus (SGF).[20,21] However, the quantitative relationship between HCF and the degree of fundus pigmentation has not yet been elucidated in detail. Therefore, in this study, we hypothesized that HCFs on en face OCT images vary with the fundus color in patients with VKH disease and would differ from those of normal subjects. We investigated the relationship between HCF on en face OCT images and the degree of fundus pigmentation in eyes with normal fundus and VKH disease. We also comparatively analyzed the differences in HCF distribution in VKH disease-affected eyes with and without SGF, as well as those of normal controls.

Methods

This retrospective study was approved by the institutional Review Board of the Korea University Anam Hospital, Seoul, Korea (IRB number: 2021AN0525), and conducted in accordance with the tenets of the Declaration of Helsinki. We reviewed the medical records of consecutive patients diagnosed with acute VKH disease between May 2016 and

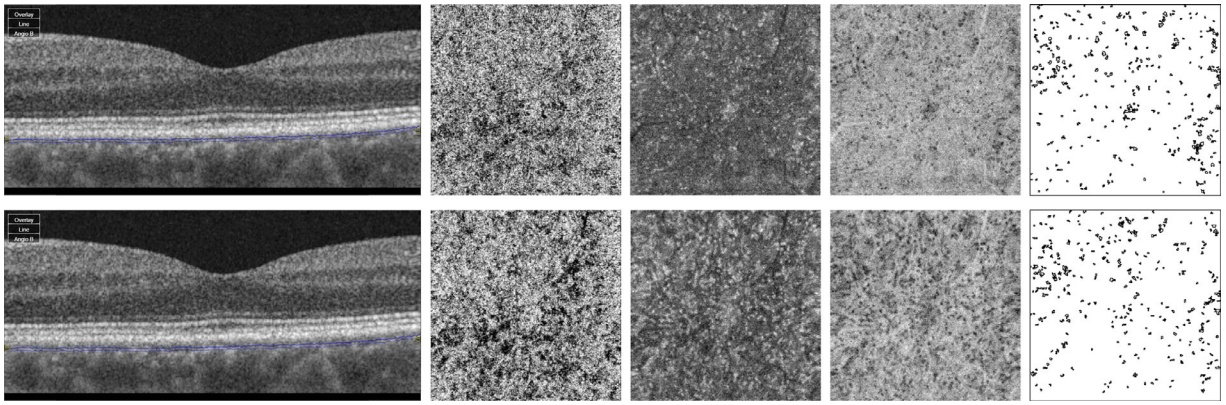

Figure 1. Measurement of hyperreflective foci on en face OCT. (**First column**) Cross-sectional SS-OCT B-scans showing the position of selected choroidal slabs (*blue line*). Two 10-μm-thick choroidal layer slabs were obtained at 10.4 to 20.8 μm below the BM (**upper row**) and at 20.8–31.2 μm below the (**lower row**). (**second column**) En face SS-OCT angiography images obtained from each corresponding slabs. (**Third column**) En face SS-OCT images before image analysis. Hyperreflective choroidal foci that appear as bright spots could be found. (**Fourth column**) Inverted en face SS-OCT images showing hyperreflective choroidal foci as dark spots. En face OCT images were reversed black/white and converted to 8-bit images using ImageJ. (**Fifth column**) Analyzed hyperreflective foci using ImageJ. *Black spots* with reflectivity below 2 standard deviations from the mean reflectivity and an area $\geq$314 μm^2 were traced using the analyzed particle tool in ImageJ.

October 2021. During the initial episode, each patient was diagnosed with VKH disease based on the revised diagnostic criteria for VKH disease[22] after a comprehensive ophthalmic examination, including slit-lamp biomicroscopy, fundoscopy, color fundus photography, fluorescein angiography, indocyanine green angiography, swept-source OCT (SS-OCT), and OCT angiography (OCTA). In the acute uveitic stage, all patients were treated with high-dose intravenous (methylprednisolone, 1000 mg/day for three days) or oral (1.0–1.5 mg/kg/d) corticosteroid therapy, followed by a slow tapering (2.5–10 mg/wk) with oral corticosteroids over a period of six to nine months. All but two patients received an additional immunosuppressive agent (cyclosporine or mycophenolate mofetil) from the initial episode or after disease recurrence. During the follow-up period, each patient underwent a comprehensive ophthalmic examination, which included slit-lamp biomicroscopy, fundus examination, color fundus photography, SS-OCT, and OCTA, but not fluorescein angiography and indocyanine green angiography.

For the analysis, we selected OCT images obtained from patients in the convalescent stage of the disease without active inflammatory signs. When several OCT images were available, we selected those obtained at the last visit. All eyes with VKH disease were divided into SGF-positive and SGF-negative groups based on clinical documentation and fundus photographs. Fundus photographs were evaluated by the consensus of two retinal experts (Y.K. and J.O). As normal controls, age- and sex-matched subjects were included from the same database. We randomly selected one of the two eyes from subjects without ocular disease or included the normal fellow eyes of subjects with unilateral ocular disease such as epiretinal membrane, retinal vein occlusion, and retinal tears. All eyes in the normal control group had a best-corrected visual acuity of 20/20 or better (Snellen), and no evidence of chorioretinal and optic nerve disease, as confirmed by medical records, fundus photography, SS-OCT, and SS-OCTA. The exclusion criteria for normal controls included the presence of comorbid chorioretinal pathologies in any of both eyes, including but not limited to age-related macular degeneration, central serous chorioretinopathy, uveitis, diabetic retinopathy, hypertensive retinopathy, and high myopia (spherical equivalent ≥ -6.00 diopters). Eyes that had undergone ocular laser treatment or surgery were also excluded.

Quantification of Hyperreflective Choroidal Foci on en Face OCT Images

OCT images were obtained using DRI OCT Triton (version 10.13.003.06; Topcon Corp., Tokyo, Japan) during a OCTA macular scan protocol with a nominal scan area of 3 × 3 mm. The macular scan consisted of 320 A-scans × 320 B-scans and was obtained in the macula centered on the fovea with four repeated scans at each of the 320 different locations. Using built-in software, en face OCT images were generated as previously described[18,19] with modified slabs. Two 10-μm−thick choroidal layer slabs were selected between 10.4 and 20.8 μm and between 20.8 and 31.2 μm below the Bruch's membrane (BM). We defined HCF as small, hyperreflective, well-circumscribed dots or spots on en face OCT images. For quantitative measurement and noise reduction, the threshold of HCF reflectivity was determined at two standard deviations above the mean reflectivity of each en face OCT image as previously described.[18,19] We analyzed the distribution of HCFs that had higher reflectivity than this threshold with an area $\geq$314 μm^2 using ImageJ software (version 1.53m; National Institutes of Health, Bethesda, MD, USA; http://imagej.nih.gov/ij) (Fig. 1).[18,19] In brief, after the black-and-white inversion of the en face OCT images, each was converted to an eight-bit image in ImageJ. The mean and standard deviation of the reflectivity of the en face images in each slab were measured using the image histogram tool, and the threshold level was determined. After this threshold was applied as the upper limit, the images were binarized using a default setting. Then, a watershed function was used to reduce noise that makes the two small spots appear to be connected. Next, the analyze particle tool was used to trace the HCF boundaries. The numbers and total areas of the HCFs were calculated.

Degree of Fundus Pigmentation

The degree of fundus pigmentation was determined objectively by the color balance of the fundus photographs, as

Investigative Ophthalmology & Visual Science

previously described in patients with VKH disease.[23–25] The color balance was quantified using a color fundus photograph that was acquired concurrently with the OCT scan using a fundus camera incorporated in the OCT device. The degree of fundus pigmentation was determined in the macular center and nasal perifoveal area between the fovea and the optic disc, covering a nominal 3 × 3 mm area, by modifying the measurement area from the previous method.[23–25] The RGB stack tool was used to separate the color fundus images into red (R), green (G), and blue (B) channels. After histogram generation, the mean intensities of each color channel were measured.[18,23–25] The degree of fundus pigmentation was then calculated as R/(R + G + B) according to the method described as the "sunset glow index" in previous studies.[23–25]

Statistical Analysis

Categorical variables were compared using the Fisher's exact tests. Continuous variables were compared using the generalized estimation equations (GEE) to account for the correlation between the eyes of the same patient. For multiple comparison tests, we performed GEE, followed by a sequential Holm–Bonferroni correction for pairwise comparison. The correlation between the HCF and various parameters was assessed using Spearman's correlation coefficient (ρ). The χ^2 test and GEE were performed using IBM SPSS Statistics for Windows (version 20.0; IBM Corp., Armonk, NY, USA). And the correlation between variables was analyzed and plotted using GraphPad Prism for Windows (version 9.3.1; GraphPad Software, San Diego, CA, USA). A P value <0.05 was considered to be statistically significant.

Results

General Characteristics

Twenty-two eyes of 11 patients with VKH disease and 22 eyes with normal fundus from 22 age- and sex-matched normal controls were included, and the baseline characteristics of the included subjects are summarized in Table 1. The median age of VKH patients and normal controls was 58.0 (range 54.0–65.0) years. Median disease duration was 66.4 (range 8.5–147.7) months.

The best-corrected visual acuity (BCVA) was poorer in patients with VKH disease than in normal controls after accounting for inter-eye correlation ($P = 0.011$) (Table 2). However, spherical equivalent refractive error was not significantly different between the eyes with VKH disease and

Table 1. Demographic and Clinical Characteristics of Normal Controls and Patients with Vogt-Koyanagi-Harada Disease

Variables	Controls ($n = 22$)	Patients With VKH Disease ($n = 11$)	P Value
Number of eyes	22	22	
Age, years, median (IQR)	58.0 (54.0–65.0)	58.0 (54.0–65.0)	
Sex			
Female, n (%)	14 (64.6)	7 (64.6)	
Male, n (%)	8 (36.4)	4 (36.4)	
Hypertension, n (%)	8 (36.4)	3 (27.3)	0.709
Diabetes, n (%)	2 (9.1)	2 (18.2)	0.586
Disease duration, months, median (IQR)	n.a.	66.4 (20.1–86.1)	
Number of disease recurrence, median (interquartile range)	n.a.	1.0 (0–3.0)	
Sunset glow fundus, n (%)	n.a.	5 (45.5%)*	

n, number of subjects; VKH, Vogt–Koyanagi–Harada; IQR, interquartile range; n.a., not applicable.
P values were estimated by Fisher's exact test
* Both eyes of five patients (10 eyes) were included.

Table 2. Comparison of Baseline Characteristics, Fundus Pigmentation, and Hyperreflective Choroidal Foci Between Eyes of Normal Controls and Those With Vogt-Koyanagi-Harada Disease

Variables	Normal Controls ($n = 22$ eyes)	Eyes With VKH Disease ($n = 22$ eyes)	P Value
Spherical equivalent, diopter	–0.619 (–1.287 to 0.049)	–0.875 (–1.967 to 0.217)	0.695
Best corrected visual acuity, logMAR	0.000 (0.000–0.000)	0.226 (0.051–0.401)	0.011*
Subfoveal choroidal thickness, μm	268.2 (225.2–311.2)	269.5 (217.4–321.6)	0.970
Degree of fundus pigmentation			
At the fovea	0.563 (0.556–0.570)	0.591 (0.571–0.612)	0.009*
At the nasal perifovea	0.558 (0.551–0.565)	0.578 (0.562–0.594)	0.025*
Hyperreflective choroidal foci			
Between 10.4 and 20.8 μm below the BM			
Number	211.9 (190.3–233.4)	186.1 (151.4–220.8)	0.216
Total area, μm^2	197,234.8 (174,215.3–220,254.4)	167,295.8 (122,416.9–212,174.8)	0.245
Total area, %†	2.192 (1.936–2.447)	1.859 (1.360–2.358)	0.245
Between 20.8 and 31.2 μm below the BM			
Number	236.3 (218.8–253.7)	207.0 (176.2–237.9)	0.106
Total area, μm^2	221,353.7 (196,338.8–246,368.5)	197,086.7 (155,563.8–238,609.7)	0.327
Total area, %†	2.460 (2.182–2.737)	2.190 (1.728–2.651)	0.327

CI, confidence interval; logMAR, logarithm of the minimum angle of resolution.
Data are expressed as estimated marginal means (95% confidence interval).
* P value < 0.05 by the generalized estimation equation method to account for inter-eye correlation of a subject.
† The total area of the HCFs was calculated in percent by dividing the number of pixels with reflectivity higher than the threshold by the total number of pixels.

Investigative Ophthalmology & Visual Science

Table 3. Correlation Between the Distribution of Hyperreflective Choroidal Foci and Other Parameters in Eyes With Vogt-Koyanagi-Harada Disease

	Between 10.4 and 20.8 µm Below the BM				Between 20.8 and 31.2 µm Below the BM			
	Number of HCF		Total Area of HCF		Number of HCF		Total Area of HCF	
Variables	**ρ (95% CI)**	***P* Value**	**ρ (95% CI)**	***P* Value**	**ρ (95% CI)**	***P* Value**	**ρ (95% CI)**	***P* Value**
Age	−0.141 (−0.540 to 0.311)	0.532	−0.122 (−0.527 to 0.328)	0.589	0.034 (−0.404 to 0.460)	0.880	0.047 (−0.394 to 0.470)	0.837
Disease duration	0.233 (−0.221 to 0.605)	0.296	0.384 (−0.058 to 0.700)	0.078	0.035 (−0.404 to 0.460)	0.879	0.095 (−0.352 to 0.506)	0.676
Best-corrected visual acuity	0.003 (−0.430 to 0.435)	0.988	0.105 (−0.343 to 0.514)	0.641	−0.144 (−0.543 to 0.307)	0.521	−0.210 (−0.589 to 0.244)	0.347
Subfoveal choroidal thickness	−0.067 (−0.486 to 0.376)	0.766	−0.143 (−0.542 to 0.309)	0.526	0.079 (−0.366 to 0.495)	0.726	−0.184 (−0.571 to 0.270)	0.412
Degree of fundus pigmentation								
At the fovea	−0.671 (−0.855 to −0.336)	< 0.001*	−0.612 (−0.826 to −0.243)	0.002*	−0.414 (−0.718 to 0.023)	0.056	−0.417 (−0.720 to 0.019)	0.053
At the nasal perifovea	−0.558 (−0.798 to −0.166)	0.007*	−0.538 (−0.787 to −0.138)	0.010*	−0.147 (−0.545 to 0.305)	0.513	−0.209 (−0.589 to 0.245)	0.349

95% CI, 95% confidence interval.
ρ, Spearman's rho,
* *P* value < 0.05 by Spearman's correlation analysis.

those of normal controls. The degree of fundus pigmentation was significantly lower in VKH disease–affected eyes than in those with normal fundus both at the fovea ($P = 0.009$) and perifovea ($P = 0.025$). However, HCFs on en face images did not differ between the eyes with VKH disease and those of normal controls (all $P > 0.05$). BCVA of patients with VKH disease did not correlate with disease duration, age, degree of fundus pigmentation, or distribution of HCF.

Correlation Between HCF and Degree of Fundus Pigmentation

In patients with VKH disease, the number and area of HCF on en face images between 10.4 and 20.8 μm below the BM correlated with the degree of fundus pigmentation at the foveal center ($P = 0.001$ and $P = 0.002$, respectively) and the nasal perifovea ($P = 0.007$ and $P = 0.010$, respectively) (Table 3) (Fig. 2). However, these relationships were not significant in normal controls (Table 4).

Comparison of HCF Between VKH Disease–Affected Eyes With/Without SGF and Normal Controls

Of the 11 patients with VKH disease, SGF was observed in both eyes (10 eyes) of five patients (Tables 1 and 5). The number of HCF on en face images derived from 10.4 to 20.8 µm below the BM was significantly smaller in VKH disease–affected eyes with SGF (the estimated marginal means, 95% confidence interval [CI]: 134.6, 110.0–159.2) than in those without SGF (229.0, 197.0–261.0) or in normal controls (211.8, 190.3–233.4) ($P < 0.001$ and $P < 0.001$, respectively). The total area of HCF was similarly decreased in the eyes with SGF, in comparison to that of VKH disease–affected eyes without SGF ($P < 0.001$) and normal controls ($P = 0.001$). Although not statistically significant, a similar tendency of difference in the number ($P = 0.050$) and total area ($P = 0.115$) of HCF between the groups was observed

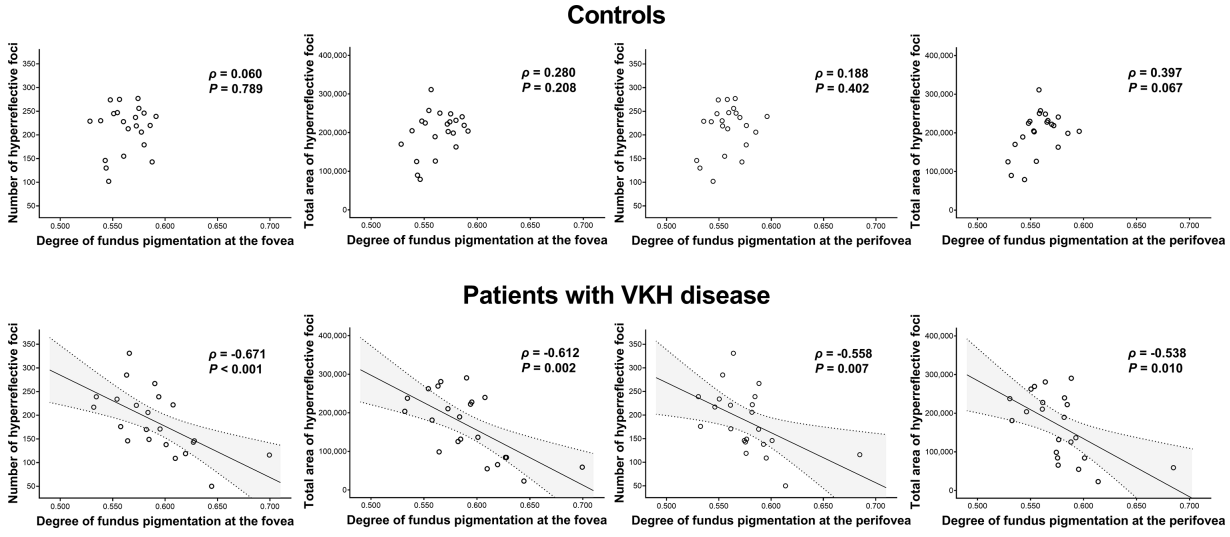

Figure 2. Scatter plots of the relationship between the hyperreflective foci in the choroid at 10.4–20.8 µm below the Bruch's membrane and the degree of fundus pigmentation at the fovea (**first and second column**) and the nasal perifovea (**third and fourth column**) in eyes of normal controls (**upper row**) and those with Vogt-Koyanagi-Harada disease (**lower row**). *Solid* and *dashed lines* represent linear regression line and 95% confidence intervals, respectively.

Investigative Ophthalmology & Visual Science

Table 4. Correlation Between the Distribution of Hyperreflective Choroidal Foci and Other Parameters in Eyes of Normal Controls

	Between 10.4 and 20.8 µm Below the BM				Between 20.8 and 31.2 µm Below the BM			
	Number of HCF		Total Area of HCF		Number of HCF		Total Area of HCF	
Variables	ρ (95% CI)	*P* Value	ρ (95% CI)	*P* Value	ρ (95% CI)	*P* Value	ρ (95% CI)	*P* Value
Age	−0.385 (−0.701 to 0.057)	0.077	−0.461 (−0.745 to −0.035)	0.031	−0.222 (−0.597 to 0.233)	0.320	−0.207 (−0.587 to 0.247)	0.354
Subfoveal choroidal thickness	0.076 (−0.368 to 0.492)	0.736	0.281 (−0.173 to 0.636)	0.206	0.429 (−0.005 to 0.727)	0.046	0.554 (0.160 to 0.796)	0.007
Degree of fundus pigmentation								
At the fovea	0.060 (−0.382 to 0.480)	0.789	0.280 (−0.174 to 0.635)	0.208	0.323 (−0.127 to 0.663)	0.142	0.399 (−0.040 to 0.709)	0.066
At the nasal perifovea	0.188 (−0.266 to 0.574)	0.402	0.397 (−0.043 to 0.708)	0.067	0.299 (−0.153 to 0.648)	0.176	0.317 (−0.134 to 0.659)	0.151

95% CI, 95% confidence interval.

ρ, Spearman's rho, *P value < 0.05 by Spearman's correlation analysis.

Table 5. Comparison of Parameters Between Vogt-Koyanagi-Harada Disease–Affected Eyes With and Without Sunset Glow Fundus

	Eyes with VKH disease				Post Hoc Pairwise Comparisons†		
Variables	With SGF (*n* = 10 Eyes)	Without SGF (*n* = 12 Eyes)	Normal Controls (*n* = 22 Eyes)	Overall *P* Value*	SGF+ Vs SGF−	SGF+ Vs Controls	SGF− Vs Controls
Age (y)	62.8 (57.1–68.5)	55.8 (48.6–63.1)	58.9 (55.1–62.8)	0.309	0.419	0.537	0.537
Disease duration (mo)	46.2 (20.7–71.7)	75.7 (37.2–114.2)	n.a.	n.a.	0.210	n.a.	n.a.
Best-corrected visual acuity, logMAR	0.192 (0.018–0.366)	0.255 (−0.029 to 0.538)	0.000 (0.000–0.000)	**0.020**	0.710	0.092	0.156
Spherical equivalent, diopter	−1.238 (−3.424 to 0.949)	−0.573 (−1.322 to 0.176)	–0.619 (–1.287 to 0.049)	0.725	> 0.999	> 0.999	> 0.999
Subfoveal choroidal thickness (µm)	277.6 (181.4–373.8)	262.8 (211.4–314.1)	268.2 (225.2–311.2)	0.963	> 0.999	> 0.999	> 0.999
Degree of fundus pigmentation							
At the fovea	0.613 (0.582–0.643)	0.574 (0.555–0.592)	0.563 (0.556–0.569)	**0.005**	0.061	**0.005**	0.268
At the nasal perifovea	0.590 (0.563–0.617)	0.568 (0.553–0.582)	0.558 (0.551–0.565)	**0.048**	0.298	0.070	0.298
Hyperreflective choroidal foci							
Between 10.4 and 20.8 µm below the BM							
Number	134.6 (110.0–159.2)	229.0 (197.0–261.0)	211.8 (190.3–233.4)	**< 0.001**	**< 0.001**	**< 0.001**	0.384
Total area, µm^2	100,511.7 (51,561.6–149,461.8)	222,949.2 (195,690.2–250,208.3)	197,234.8 (174,215.3–220,254.4)	**< 0.001**	**< 0.001**	**0.001**	0.158
Total area, %‡	1.117 (0.573–1.661)	2.477 (2.174–2.780)	2.192 (1.936–2.447)	**< 0.001**	**< 0.001**	**0.001**	0.158
Between 20.8 and 31.2 µm below the BM							
Number	172.9 (124.2–221.6)	235.4 (215.0–255.8)	236.3 (218.8–253.7)	0.050	0.049	0.049	0.951
Total area, µm^2	155,540.0 (91,832.9–219,247.2)	231,709.0 (195,817.6–267,600.4)	221,353.7 (196,338.8–246,368.5)	0.115	0.124	0.124	0.643
Total area, %‡	1.728 (1.020–2.436)	2.575 (2.176–2.973)	2.460 (2.182–2.737)	0.115	0.124	0.124	0.643

SGF+, VKH disease–affected eyes with sunset glow fundus; SGF−, VKH disease–affected eyes without sunset glow fundus; logMAR, logarithm of the minimum angle of resolution; n.a., not applicable.

Data are expressed as estimated marginal means (95% confidence interval). Bold *P* values denote statistical significance at the $P < 0.05$ level.

* *P* values were estimated using a generalized estimation equation method to account for intereye correlation of a subject.

† Adjusted *P* values were estimated using a sequential Holm–Bonferroni correction for multiple comparisons.

‡ The total area of the HCFs was calculated in percent by dividing the number of pixels with reflectivity higher than the threshold by the total number of pixels.

Table 6. Characteristics of Vogt-Koyanagi-Harada Patients With Sunset Glow Fundus

		Sunset Glow Fundus		Degree of Fundus Depigmentation at the Foveal Center		Number of HCF Between 10.4 and 20.8 mm Below the BM		Total Area of HCF Between 10.4 and 20.8 mm Below the BM, mm^2	
Subjects	Eye Site	Previous Visit	Last Visit	Previous Visit	Last Visit	Previous Visit	Last Visit	Previous Visit	Last Visit
Patient 1	Right	n.a.	Yes	n.a.	0.699	n.a.	116	n.a.	59,150
	Left	n.a.	Yes	n.a.	0.628	n.a.	146	n.a.	84,287
Patient 2	Right	Yes	Yes	0.556	0.564	152	146	98,438	98,789
	Left	Yes	Yes	0.569	0.582	147	170	94,658	125,596
Patient 3	Right	Yes	Yes	0.664	0.627	94	143	62,842	84,375
	Left	Yes	Yes	0.612	0.644	163	50	98,701	23,115
Patient 4	Right	No	Yes	0.587	0.619	143	119	76,377	65,654
	Left	No	Yes	0.588	0.61	156	109	101,338	55,020
Patient 5	Right	Yes	Yes	0.563	0.558	182	176	168,398	181,230
	Left	Yes	Yes	0.608	0.595	172	171	153,984	227,900

n.a., not available.

Investigative Ophthalmology & Visual Science

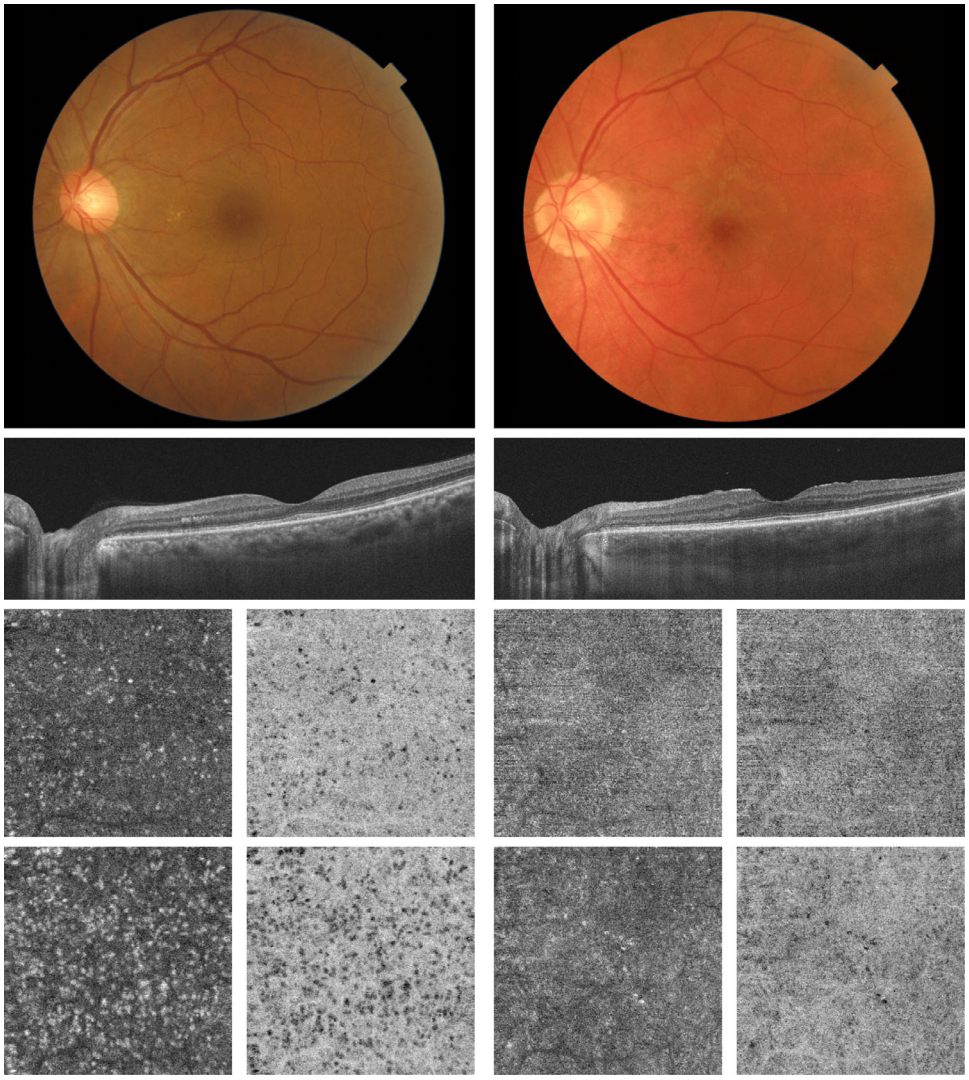

Figure 3. Fundus photographs and en face optical coherence tomography images of a 58-year-old man with Vogt-Koyanagi-Harada disease at two months (*left column*) and 68 months (*right column*) after the first attack.

on en face images derived from 20.8 and 31.2 µm below the BM.

Cases of Eyes with Sunset Glow Fundus

For eight of the 10 eyes that showed SGF at the last visit, OCT images obtained at different times during the convalescent stage were available (Table 6). The median interval between the previous and last visit was 22.3 (range 6.6–34.8) months. Two of these eyes from one patient did not show SGF at the previous visit (Fig. 3). However, at the last visit at 68 months, the degree of pigmentation on fundus photographs had increased above 0.6, and the number of HCF on OCT images had decreased below 200.

Discussion

The effect of VKH disease on the choroid is characterized by variable degrees of choroidal hypopigmentation during the convalescent or chronic recurrent stages of VKH disease.[1,2] The degree of fundus pigmentation was attempted to be measured using color fundus photography to evaluate choroidal involvement in previous studies.[23,24] In the current study using en face OCT images, we evaluated the presence and distribution of HCF in the inner choroid. We found that the distribution of HCF on en face OCT images correlated with the degree of fundus pigmentation, which was measured using the color balance of the fundus photographs. This finding suggests that variations in HCF are related to cellular abnormalities in the choroid in VKH disease. Histopathologically, inflammatory cell populations in the choroid vary according to disease stage.[3,8–10] In the acute stage, non-necrotizing granulomatous inflammation with peripheral diffuse and heavy lymphocyte infiltration surrounding central aggregates of multinucleated giant and epithelioid cells containing melanin pigment granules causes thickening of the choroid.[1,9,10] In the convalescent stage, less -severe nongranulomatous inflammation consisting of lymphocytes and plasma cells is observed.[1,9,10] Although the retinal pigment epithelium is relatively well preserved with or without focal injury, loss of melanin granules of choroidal melanocytes from an autoimmune process results in SGF,[9,20] which is associated with a poor prognosis

Investigative Ophthalmology & Visual Science

in some patients.[2,26] Variations in the distribution of HCF in our patients may be related to some of these cellular abnormalities in the choroid.

Several studies have reported on the origin of hyperreflective foci on OCT images. Some previous studies suggested macrophages to be candidates for the origin of hyperreflective foci in diabetic retinopathy.[15,27] Bolz et al.[14] showed that lipid exudation could be attributed to hyperreflective foci. Spaide et al.[28] proposed that it is related to the packing density of collagen fibers. In a previous study using OCT B-scan images, Fong et al.[29] observed that hyperreflectivity foci in the inner choroid were reduced in patients with VKH disease as compared to age-matched healthy controls in both the acute and convalescent stages. The authors suggested that hyperreflective foci in the choroid could be attributed to cross-sectional views of pericapillary arterioles and venules. However, Kim and Oh[18] demonstrated the presence of hyperreflective foci in the normal choroid of healthy subjects as well, and suggested that they could be related to melanin pigmentation. In a previous study using OCT, Huang et al.[21] showed that SGF was related to choroidal depigmentation. In the current study, we found that eyes with SGF had lower numbers and smaller total areas of HCF than those without. This result suggests that HCF could originate from pigments in melanocytes, which is important in the development and progression of VKH disease. Another possibility is that these HCF variations are related to the resolution of inflammatory cells, which are recruited during the acute stage of VKH disease. However, in the current study, the distribution of HCF in VKH disease-affected eyes without SGF was not different from that observed in healthy controls. This suggests that the differences in inflammatory cell populations may not have a significant effect on HCF distribution.

In the diagnosis and monitoring of chronic VKH disease, determining the presence and development of SGF is important.[2,3,30] However, subjective fundus examination is still used to determine its presence. Several studies have used color balance measurements on fundus photographs to objectively evaluate fundus alterations in VKH patients.[23,24] In this study, the degree of fundus pigmentation measured using fundus photographs showed significant differences between normal controls and patients with VKH disease. However, previous studies reported that the color balance of fundus photographs is affected by choroid thickness, media opacity, and imaging artifacts, and limitations exist in determining whether SGF develops in patients with VKH disease.[24,31,32] Consistent with previous studies,[24,31,32] in the present study, the degree of fundus pigmentation did not differ between VKH disease–affected eyes with and without SGF, nor between the eyes of normal controls and VKH disease–affected eyes without SGF. Using en face OCT images, the number and total area of HCF in VKH disease–affected eyes with SGF were significantly lower than those in VKH disease–affected eyes without SGF and normal controls. These findings suggested that quantitative measurement of HCF on en face OCT could be a useful objective tool for detecting SGF.

In previous studies, variation of reflectivity on OCT images has been studied on B-scan images.[29] High resolution obtained by averaging B-scan images makes it possible to better delineate abnormal regions with hyper- or hyporeflectivity. We used en face images to determine the distribution of HCF. The en face OCT images were derived from the OCT volumetric data obtained during an OCTA scanning protocol, where each B-scan was repeated four times at the same location. This scanning protocol would have rendered HCF more distinct, even on en face images. In the current study, we selected two inner choroidal slabs for en face images. Previous studies[33,34] have suggested that melanin pigmentation can prevent light penetration into the outer choroidal layer and thus prevent visibility of the deep choroidal structures. This could then hinder choroidal measurements using en face images in the deep choroidal layer. Although the ideal location for the delineation of choroidal pigmentation may vary with OCT devices, by using the inner choroidal slabs, we were able to measure HCF quantitatively in a two-dimensional area.

This study has several limitations, including its retrospective design and the small number of cases studied. Due to the small number of cases and inclusion of both eyes of patients, stratification for further analysis was not possible. This study compared the quantitative measurements on OCT images and fundus photographs between age- and sex-matched healthy controls and patients with VKH disease. However, we could not analyze the longitudinal changes in all cases. Further longitudinal studies over several years are warranted to better understand the relationship between HCF and progressive changes in choroidal pigmentation. Additionally, we were unable to adjust the measurements obtained from the en face OCT images according to axial length. Although there was no difference in refractive errors between the groups in this study, the magnification effect caused by the difference in axial length of subjects could have influenced the total area measurements of HCFs. This inaccuracy in the HCF area measurements from individual subjects may have an impact on our results, and care should be taken into consideration when interpreting our results. Current study in patients with SGF caused by VKH supports the suggestion that HCF can originate from the pigmentation of melanocytes in the choroid.[18,19] However, we were also unable to directly compare the distribution of HCF on en face OCT images with histologic examination and other imaging modalities such as near-infrared and autofluorescence images. Further studies that include cases at various stages of the disease, multimodal imaging, and histopathologic studies could help elucidate the variations in HCF as well as visual prognoses.

In conclusion, we found that the distribution of HCF correlated with the degree of fundus pigmentation in eyes with VKH disease. A decrease in the number of HCF was apparent in VKH disease–affected eyes with SGF. Quantitative measurements of HCF on en face OCT images can be a novel tool in evaluating choroidal pigmentation in patients with VKH disease.

Acknowledgments

Supported by a Korea Medical Device Development Fund grant funded by the Korean government (Ministry of Science and ICT; Ministry of Trade, Industry and Energy; Ministry of Health & Welfare; and Ministry of Food and Drug Safety) (NTIS Number: 1711137942, KMDF_PR_20200901_0026).

Disclosure: **Y.H. Kim,** None; **A. Togloom,** None; **J. Oh,** None

References

1. Lavezzo MM, Sakata VM, Morita C, et al. Vogt-Koyanagi-Harada disease: review of a rare autoimmune disease targeting antigens of melanocytes. *Orphanet J Rare Dis*. 2016;11:29.

2. Herbort CP, Jr., Tugal-Tutkun I, Abu-El-Asrar A, et al. Precise, simplified diagnostic criteria and optimised management of initial-onset Vogt-Koyanagi-Harada disease: an updated review. *Eye (Lond).* 2022;36:29–43.
3. Moorthy RS, Inomata H, Rao NA. Vogt-Koyanagi-Harada syndrome. *Surv Ophthalmol.* 1995;39:265–292.
4. Spaide RF, Koizumi H, Pozzoni MC. Enhanced depth imaging spectral-domain optical coherence tomography. *Am J Ophthalmol.* 2008;146:496–500.
5. Agrawal R, Li LK, Nakhate V, Khandelwal N, Mahendradas P. Choroidal vascularity index in Vogt-Koyanagi-Harada disease: An EDI-OCT derived tool for monitoring disease progression. *Transl Vis Sci Technol.* 2016;5(4):7.
6. Aggarwal K, Agarwal A, Mahajan S, et al. The role of optical coherence tomography angiography in the diagnosis and management of acute Vogt-Koyanagi-Harada disease. *Ocul Immunol Inflamm.* 2018;26:142–153.
7. Liu S, Du L, Zhou Q, et al. The choroidal vascularity index decreases and choroidal thickness increases in Vogt-Koyanagi-Harada disease patients during a recurrent anterior uveitis attack. *Ocul Immunol Inflamm.* 2018;26:1237–1243.
8. Perry HD, Font RL. Clinical and histopathologic observations in severe Vogt-Koyanagi-Harada syndrome. *Am J Ophthalmol.* 1977;83:242–254.
9. Rao NA. Pathology of Vogt-Koyanagi-Harada disease. *Int Ophthalmol.* 2007;27(2-3):81–85.
10. Inomata H, Rao NA. Depigmented atrophic lesions in sunset glow fundi of Vogt-Koyanagi-Harada disease. *Am J Ophthalmol.* 2001;131:607–614.
11. Piri N, Nesmith BL, Schaal S. Choroidal hyperreflective foci in Stargardt disease shown by spectral-domain optical coherence tomography imaging: correlation with disease severity. *JAMA Ophthalmol.* 2015;133:398–405.
12. Roy R, Saurabh K, Shah D, Chowdhury M, Goel S. Choroidal hyperreflective foci: a novel spectral domain optical coherence tomography biomarker in eyes with diabetic macular edema. *Asia Pac J Ophthalmol (Phila).* 2019;8:314–318.
13. Romano F, Arrigo A, MacLaren RE, et al. Hyperreflective doci as a pathogenetic biomarker in choroideremia. *Retina.* 2020;40:1634–1640.
14. Bolz M, Schmidt-Erfurth U, Deak G, et al. Optical coherence tomographic hyperreflective foci: a morphologic sign of lipid extravasation in diabetic macular edema. *Ophthalmology.* 2009;116:914–920.
15. Ong JX, Nesper PL, Fawzi AA, Wang JM, Lavine JA. Macrophage-like cell density Is increased in proliferative diabetic retinopathy characterized by optical coherence tomography angiography. *Invest Ophthalmol Vis Sci.* 2021;62(10):2.
16. Coscas G, De Benedetto U, Coscas F, et al. Hyperreflective dots: a new spectral-domain optical coherence tomography entity for follow-up and prognosis in exudative age-related macular degeneration. *Ophthalmologica.* 2013;229:32–37.
17. Schreur V, Altay L, van Asten F, et al. Hyperreflective foci on optical coherence tomography associate with treatment outcome for anti-VEGF in patients with diabetic macular edema. *PLoS One.* 2018;13(10):e0206482.
18. Kim YH, Oh J. Hyperreflective foci in the choroid of normal eyes. *Graefes Arch Clin Exp Ophthalmol.* 2022;260:759–769.
19. Kim YH, Oh J. Comparison of choroidal hyperreflective spots on optical coherence tomography images between both eyes of normal subjects. *Quant Imaging Med Surg.* 2022;12:920–935.
20. Inomata H, Sakamoto T. Immunohistochemical studies of Vogt-Koyanagi-Harada disease with sunset sky fundus. *Curr Eye Res.* 1990;9(Suppl):35–40.
21. Huang Y, Yang YT, Lin B, et al. Melanin change of retinal pigment epithelium and choroid in the convalescent stage of Vogt-Koyanagi-Harada disease. *Int J Ophthalmol.* 2020;13:1928–1932.
22. Read RW, Holland GN, Rao NA, et al. Revised diagnostic criteria for Vogt-Koyanagi-Harada disease: report of an international committee on nomenclature. *Am J Ophthalmol.* 2001;131:647–652.
23. Suzuki S. Quantitative evaluation of "sunset glow" fundus in Vogt-Koyanagi-Harada disease. *Jpn J Ophthalmol.* 1999;43:327–333.
24. Komuku Y, Ishikawa H, Ide A, et al. Predictive biomarker for progression into the sunset glow fundus of Vogt-Koyanagi-Harada disease, using adaptive binarization of fundus photographs. *Transl Vis Sci Technol.* 2020;9(11):10.
25. Yoshihara N, Yamashita T, Ohno-Matsui K, Sakamoto T. Objective analyses of tessellated fundi and significant correlation between degree of tessellation and choroidal thickness in healthy eyes. *PLoS One.* 2014;9(7):e103586.
26. Keino H, Goto H, Usui M. Sunset glow fundus in Vogt-Koyanagi-Harada disease with or without chronic ocular inflammation. *Graefes Arch Clin Exp Ophthalmol.* 2002;240:878–882.
27. Uji A, Murakami T, Nishijima K, et al. Association between hyperreflective foci in the outer retina, status of photoreceptor layer, and visual acuity in diabetic macular edema. *Am J Ophthalmol.* 2012;153:710–717.
28. Spaide RF, Ledesma-Gil G, Mullins RF. Varying optical coherence tomography appearance of the inner choroid with age: possible explanation and histologic correlate. *Retina.* 2021;41:1071–1075.
29. Fong AH, Li KK, Wong D. Choroidal evaluation using enhanced depth imaging spectral-domain optical coherence tomography in Vogt-Koyanagi-Harada disease. *Retina.* 2011;31:502–509.
30. Herbort CP, Jr., Abu El Asrar AM, Yamamoto JH, et al. Reappraisal of the management of Vogt-Koyanagi-Harada disease: sunset glow fundus is no more a fatality. *Int Ophthalmol.* 2017;37:1383–1395.
31. Miura M, Makita S, Yasuno Y, et al. Polarization-sensitive optical coherence tomographic documentation of choroidal melanin loss in chronic Vogt-Koyanagi-Harada disease. *Invest Ophthalmol Vis Sci.* 2017;58:4467–4476.
32. Miura M, Makita S, Yasuno Y, et al. Objective evaluation of choroidal melanin loss in patients with Vogt-Koyanagi-Harada disease using polarization-sensitive optical coherence tomography. *Sci Rep.* 2022;12:3526.
33. Yiu G, Vuong VS, Oltjen S, et al. Effect of uveal melanocytes on choroidal morphology in rhesus macaques and humans on enhanced-depth imaging optical coherence tomography. *Invest Ophthalmol Vis Sci.* 2016;57:5764–5771.
34. Pellegrini M, Shields CL, Arepalli S, Shields JA. Choroidal melanocytosis evaluation with enhanced depth imaging optical coherence tomography. *Ophthalmology.* 2014;121:257–261.

Investigative Ophthalmology & Visual Science